**ORIGINAL ARTICLE**     **AENSI PUBLICATIONS**

# The Mass-Dependent Effective Interactions Applied To Nuclear Reactions

**Isaiah Ochala[1*], Joseph O. Fiase[2], Vivian O. Obaje[1], Virginia I. Sule[1]**

[1]Department of Physics, Faculty of Natural Sciences, Kogi State University, Anyigba, Nigeria
[2]Department of Physics, Faculty of Science, Benue State University, Makurdi, Nigeria

**Correspondence Author:** Isaiah Ochala, Kogi State University, Department of Physics, Faculty of Natural Sciences, P. M. B. 1008, Anyigba, Nigeria
Email: ojoagbamiisaiah1234@gmail.com

**Cite as:** I. Ochala, J.O. Fiase, V. O. Obaje and V. I. Sule., 2021. The Mass-Dependent Effective Interactions Applied To Nuclear Reactions. Australian Journal of Basic and Applied Sciences, 15(10): 1-12. DOI: 10.22587/ajbas.2021.15.10.1.

**ABSTRACT**

Two new mass-dependent M3Y-type effective interactions derived on the basis of the lowest order constrained variational (LOCV) approach are applied to nuclear reactions in this paper. These effective interactions were derived from nuclear systems with mass numbers A = 16 and 24 and called the B3Y-Fetal and B'3Y-Fetal respectively. Principally, nuclear reaction is used in this work as a second level of viability test to determine the effect of mass dependence on the form and character of the effective interactions. The real folded potentials associated with the B3Y-Fetal and B'3Y-Fetal have been computed within the framework of double folding model, with the former as the standard for comparison. Accordingly, the real folded potential derived from the B'3Y-Fetal in its DDB'3Y1 density-dependent version (DDB'3Y1-Fetal potential) computed within the framework of the double folding model at the incident energies of 160, 480, 960 and 1440 MeV at smaller inter-nuclear distances has been found to be -345, -289, -212 and -155 MeV, respectively, in magnitude in comparison with -352, -292, -217 and -156 MeV respectively obtained with the DDB3Y1-Fetal real folded potential at the same incident energies, showing the B3Y-Fetal to be stronger at smaller inter-nuclear distances than the B'3Y-Fetal effective interaction. The results obtained in this work have also shown the B'3Y-Fetal-based folded potential to have attractive direct and exchange components which combine to produce an attractive total real folded potential, whereas the real folded potential derived from the B3Y-Fetal effective interaction has a repulsive direct component, which combines with a large attractive exchange component to form an attractive total real folded potential. Essentially, this shows that the effect of mass dependence on the form and character of the B3Y-Fetal and B'3Y-Fetal lies in the direct components of their optical potentials.

**Keywords:** Mass-dependent, Effective interactions, B'3Y-Fetal, Double folding, Nuclear reactions

## INTRODUCTION

The mass-dependent effective interactions of the M3Y type were derived from the core systems A = 16, 24, 40 and 90 based on the Low-Order Constrained Variational (LOCV) approach in 2002 (Fiase et al., 2002), but their applications weren't studied straight away at the time. However, one of the strong bases for discussing their strengths and weaknesses is to examine their applications, one of which is a core matter. Mainly, symmetric nuclear matter (SNM), as a testing ground (Bohr and Mottelson, 1969) for effective interactions, presents a solid basis for determining the strengths and weaknesses of the new mass-dependent interactions. . Since this was well known, this nuclear matter was used in earlier work as a starting point to determine the viability of the effective interactions (Ochala et al., 2020). Accordingly, it was reported in that paper that the B3Y-Fetal, B'3Y-Fetal, B*3Y-Fetal and B†3Y-Fetal effective interactions, based on nuclear systems A = 16, 24, 40 and 90 respectively, predicted the binding energies, $\varepsilon$ = 15.2, 14.5, 11.2 and 8.2 MeV, respectively, for SNM at the saturation density, $\rho_0$ = 0.17fm$^{-3}$. These results of (Ochala et al., 2020) have shown the B3Y-Fetal and B'3Y-Fetal effective interactions, based on the nuclear systems A = 16 and 24, respectively, to give an accurate description of the binding energy per nucleon ($\varepsilon$ = 16.0±1 MeV) of SNM at the saturation density, $\rho_0$ = 0.17$fm^{-3}$. In contrast, the B*3Y-Fetal and B†3Y-Fetal effective interactions, based on nuclear systems with A = 40

Australian Journal of Basic and Applied Sciences
ISSN: 1991-8178, EISSN: 2309-8414
Journal home page: www.ajbasweb.com

and 90 respectively, have failed to give an accurate description of nuclear matter properties at saturation. Nuclear matter calculations have shown the decreasing values of binding energy per nucleon, obtained with the various effective interactions, with increasing mass number, A (Ochala et al., 2020) to be due to the mass dependence of the effective interactions. This is the first level of viability test.

This work is based on one's strong conviction that nuclear matter alone is not a sufficient test for the viability of effective interaction. Thus, having subjected all the mass-dependent effective interactions to nuclear matter calculations in (Ochala et al., 2020), the two most viable mass-dependent effective interactions, the B3Y-Fetal and B'3Y-Fetal, are to be applied to nuclear reactions in this work, with the B'3Y-Fetal effective interaction as the essential, new element. The B3Y-Fetal effective interaction has been successfully used in nuclear matter calculations (Ochala and Fiase, 2018; Ochala et al., 2019) and nuclear reactions (Ochala et al., 2020a; Ochala, 2021) in which it demonstrated excellent agreement with the M3Y-Reid and M3Y-Paris effective interactions. For this reason, it is used as a standard with which the B'3Y-Fetal is compared in this study. This application of the B'3Y-Fetal to nuclear reaction is its second level of viability test.

In this study, the mass-dependent interactions are applied to nuclear reaction involving light heavy ions within the framework of double folding model to calculate their real optical potentials. The main objective of this paper is to determine the effect of mass dependence on the form and character of the B'3Y-Fetal in nuclear reactions compared with the B3Y-Fetal.

To do this, the direct and exchange components of the real folded potential (optical potential) derived from the B'3Y-Fetal will be computed in $^{16}O + ^{16}O$ nuclear reaction at the incident energies of 160, 480, 960 and 1440 MeV, and compared with those of the B3Y-Fetal whose form and character in nuclear reactions are well-known (Ochala et al., 2020a; Ochala, 2021). It is hoped that the results of the folding calculation will give a better insight into the form and character of the former than the results obtained from nuclear matter calculations (Ochala et al., 2020a).

Additionally, it is intended to show the similarity of the optical potentials derived from the B'3Y-Fetal, which is the fundamental, new element in the present paper, to those of the M3Y-Reid effective. This is done believing that Physics, like all of Sciences, is an arena of methodologies and methods, some of which are used to solve a similar problem with the intention to advance the frontiers of knowledge. The lowest order constrained variational (LOCV) method and the G-matrix method are two of such methods in Nuclear Physics. The LOCV method parallels the G-matrix method in terms of derivation of effective interactions. Since the new mass-dependent M3Y-type interaction is representative of the lowest order constrained variational (LOCV) method, whereas the M3Y-Reid effective interaction is representative of the G-matrix approach; this study is meant to subtly determine the goodness of the LOCV theoretical model by applying the B'3Y-Fetal effective interaction to the study of nuclear reaction.

This paper is organized such that Section 2 discusses the functional forms of the mass-dependent effective interactions and double folding formalism, whereas Section 3 is focussed on results discussion, and Section 4 makes concluding remarks.

## THE MASS-DEPENDENT INTERACTIONS IN NUCLEAR REACTION

The mass-dependent interactions are effective variational interactions derived from the lowest order constrained variational approach (Fiase et al., 2002). Their matrix elements were calculated on a harmonic oscillator basis, and the details of the calculation were reported in (Fiase et al., 2002) and in our earlier paper, in which one of them was applied to SNM calculations (Ochala and Fiase, 2018). In this paper, one uses the isoscalar part of the effective interactions (Fiase et al., 2002), whose functional forms in terms of three Yukawas are:

B'3Y-Fetal:

$$v^D(r) = \frac{6591.54e^{-4r}}{4r} - \frac{1777.55e^{-2.5r}}{2.5r}$$

$$v^{EX}(r) = \frac{6158.09e^{-4r}}{4r} - \frac{2253.33e^{-2.5r}}{2.5r} - \frac{7.8474e^{-07072r}}{0.7072r} \qquad (1)$$

B3Y-Fetal:

$$v^D(r) = \frac{10472.13e^{-4r}}{4r} - \frac{2203.11e^{-2.5r}}{2.5r}$$

$$v^{EX}(r) = \frac{499.63e^{-4r}}{4r} - \frac{1347.77e^{-2.5r}}{2.5r} - \frac{7.8474e^{-07072r}}{0.7072r} \qquad (2)$$

To reproduce the saturation properties of the cold symmetric nuclear matter within Hartree-Fock approximation (HF) (Loan et al., 2016; Tan et al., 2021) and satisfy the requirement for folding calculation, these effective interactions are used in this paper in the energy- and density-dependent form (Khoa and Oertzen, 1995; Gontcharn et al., 2004):

$$v^{D(EX)}(E, \rho, r) = g(E)F(\rho)v^{D(EX)}(r), \qquad (3)$$

Where $F(\rho)$ is the density-dependent factor and $g(E) \sim 1-0.002E$ for the M3Y- Reid (Khoa and Oertzen, 1995) and Mass-dependent interactions (Ochala et al., 2020a; Ochala, 2021); and E is the incident nucleon energy. The isoscalar energy- and density-dependent interaction of equation (3) has been tested and found to work well in folding model analyses of refractive α-nucleus (Khoa and Oertzen, 1995) and nucleus-nucleus (Khoa et al., 1994; Gontcharn et al., 2004) elastic scattering.

The explicit forms of $F(\rho)$ used in this study are (Khoa et al., 1994; Ochala et al., 2020a):

$$F(\rho) = C(1 + Ae^{-B\rho}) \qquad (4)$$

for the DDM3Yn (n = 1) interaction and

$$F(\rho) = C(1 - A\rho^B) \qquad (5)$$

for the BDM3Yn (n = 0, 1, 2, 3) interaction. The parameters $C$, $A$ and $B$ of the density dependences are such that they reproduce the saturation properties of nuclear matter at density $p_0 = 0.17 \ fm^{-3}$ with a binding energy $\varepsilon = 16$ MeV within HF calculations.

For calculating nuclear matter saturation properties, the B'3Y-Fetal interaction has been successfully used (Ochala et al., 2020) in the DDM3Yn and BDM3Yn density-dependent versions, with results that demonstrated good agreement with the B3Y-Fetal interaction. For clarity, the results obtained from nuclear matter calculations using the computer code CNMMAP in (Ochala et al., 2020) are reproduced in Table 1.

**Table 1:** Parameters of Density Dependence and Nuclear Incompressibilities Obtained with the B3Y-Fetal and B'3Y-Fetal at Saturation Density.

| Density Dependent Version | $C$ | $A$ | $B$ | K[MeV] |
|---|---|---|---|---|
| DDB3Y1-Fetal | 0.2986 | 3.1757 | 2.9605 | 176 |
| DDB'3Y1-Fetal | 0.3483 | 2.4634 | 2.9605 | 165 |
| BDB3Y0-Fetal | 1.3045 | 1.0810 | 2/3 | 196 |
| BDB'3Y0-Fetal | 1.3047 | 1.0990 | 2/3 | 183 |
| BDB3Y1-Fetal | 1.1603 | 1.4626 | 1 | 235 |
| BDB'3Y1-Fetal | 1.1676 | 1.4534 | 1 | 219 |
| BDB3Y2-Fetal | 1.0160 | 4.9169 | 2 | 351 |
| BDB'3Y2-Fetal | 1.0417 | 4.6098 | 2 | 327 |
| BDB3Y3-Fetal | 0.9680 | 20.250 | 3 | 467 |
| BDB'3Y3-Fetal | 0.9938 | 23.491 | 3 | 434 |

The equations of state of cold symmetric nuclear matter, obtained with the DDB'3Y1-, BDB'3Y0-, BDB'3Y1-, BDB'3Y2- and BDB'3Y3-Fetal interactions in Table 1, have been found to have incompressibilities $K_0$ = 165, 183, 219, 327 and 434 MeV respectively (Ochala et al., 2020). These interactions have reproduced the saturation of nuclear matter at density, $\rho = 0.17 \text{fm}^{-3}$ and binding energy per nucleon, $\varepsilon = 16$ MeV correctly. The DDM3Y1 and BDM3Y1 versions of the B'3Y-Fetal have given for SNM at equilibrium incompressibility $K_0 \sim 165 - 219$ MeV in comparison with $K_0 \sim 176 - 235$ MeV and $K_0 \sim 171 - 232$ MeV predicted by the same versions of B3Y-Fetal and M3Y-Reid effective interactions, respectively, in (Khoa and Oertzen, 1995). Comparing this with the experimental estimate of $K_0$ = 200 - 350 MeV based on studies on giant monopole resonances (Shlomo and Youngblood, 1994; Colo and Giai, 2004) and the theoretical estimate of $K_0 = 220 \pm 50$ MeV based on non-relativistic mean-field model for SNM, the prediction of B'3Y-Fetal interaction is in good agreement. This provides one with a good basis to apply it within the framework of the double folding model to compute the direct and exchange components of the associated real folded potential as a means of determining the effect of mass dependence.

In the double folding model, the direct and exchange parts of the real folded potential are obtained by folding the densities of the projectile and target nuclei with the direct and exchange components of the effective nucleon-nucleon (NN) interaction as presented in equations (6) and (7) respectively (Chien et al., 2015; Khoa et al., 2016):.

$$V_D(E, \mathbf{R}) = \int \rho_1(\mathbf{r_1})\rho_2(\mathbf{r_2})v^D(\rho, E, \mathbf{s})d\mathbf{r_1}d\mathbf{r_2} \qquad (6)$$

with $\mathbf{s} = \mathbf{r_1} - \mathbf{r_2} + \mathbf{R}$

$$V_{EX}(E, \mathbf{R}) = \int \rho_1(\mathbf{r_1}, \mathbf{r_1} + \mathbf{s})\rho_2(\mathbf{r_2}, \mathbf{r_2} - \mathbf{s})v^{EX} \times \exp\frac{[i\mathbf{K(R)s}]}{M}d\mathbf{r_1}d\mathbf{r_2} \qquad (7)$$

Where $v^D$ and $v^{EX}$ are the direct and potential exchange components of the effective interaction, $\rho_1$ and $\rho_2$ are the densities of the interacting nuclei, $\mathbf{s}$ is a vector corresponding to the distance between two specified interacting points of the projectile and target whose radius vectors are $\mathbf{r_1}$ and $\mathbf{r_2}$ respectively, and $\mathbf{R}$ denotes the vector joining the centers of mass of the two nuclei. For clarity, the geometry of the folding model is shown in Figure 1.
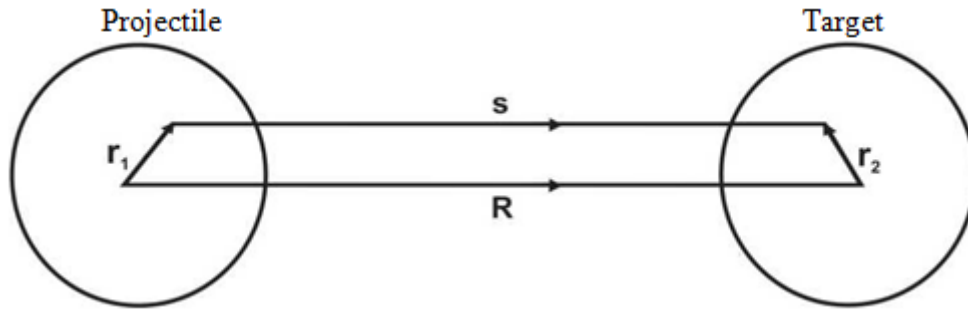


Figure 1: Geometry of Folding Model

This paper uses the isoscalar component of the density- and energy-dependent B'3Y-Fetal interaction for the folding calculation of the real optical potential because the nuclear system considered involves spin-saturated nuclei. Specifically, the B'3Y-Fetal is used in its DDM3Y1 version and the B3Y-Fetal interaction for the folding calculation following (Khoa et al., 1994; Khoa et al., 2016) to determine and compare the performance of the former with the latter.

The direct component of the folded potential is local in co-ordinate space, whereas the exchange is non-local due to the effect of anti-symmetrization occasioned by the single-nucleon knock-on exchange, which makes its evaluation difficult. Consequently, in this work, the study of real optical potential derived from the B'3Y-Fetal at various incident energies is carried out using the finite-range evaluation of the exchange potential using local momentum approximation proposed by Brieva and Rook (Brieva and Rook, 1977). Accordingly, the exact, consistent microscopic approximation to the exchange potential developed by Khoa *et al.* (Khoa et al., 1994), which produces an accurate local approximation, is employed in this work. Their approach produces an accurate local approximation. The evaluation of the non-local exchange to have a local equivalent is done by calculating the mixed density matrix, which depends on two spatial points. This is achieved by using the density matrix expansion method (Khoa et al., 1994; Hamada et al., 2012):

$$\rho(\mathbf{R}, \mathbf{R} + \mathbf{s}) \sim \rho\left(\mathbf{R} + \frac{\mathbf{s}}{2}\right)j_1\left(k_F\left(\mathbf{R} + \frac{\mathbf{s}}{2}\right)s\right) \qquad (8)$$

where $j_1(x) = 3(\sin x - x\cos x)/x^3$.

Also, a further step to take to calculate the double-folding potential is to specify the overlap density, $\rho$ of the two interacting nuclei appearing in equation (3).

For this purpose, the frozen density approximation (FDA), which corresponds to the sum of the densities of the nuclei at the mid-point of inter-nucleon separation, is adopted in the folding procedure in the form:

$$F(\rho) = F\left[\rho_1\left(\mathbf{r_1} + \frac{\mathbf{s}}{2}\right) + \rho_2\left(\mathbf{r_2} - \frac{\mathbf{s}}{2}\right)\right] \qquad (9)$$

Finally, the exchange potential is computed iteratively in this work, and a careful and accurate evaluation of the knock-on exchange effects is ensured to obtain a realistic energy dependence of the real folded potential V(E,R). The computation of the real folded potential derived from each effective interaction in this paper is carried out with the double folding model (DFM) code written by Khoa (Khoa et al., 1994 )

## RESULTS AND DISCUSSION

The results obtained with the B'3Y-Fetal effective interaction, shown in Figure 2, have been found to demonstrate good agreement with past work done with M3Y-type effective interactions such as the B3Y-Fetal, M3Y-Reid, and M3Y-Paris effective interactions.

The real folded potential, derived from the B'3Y-Fetal effective interaction, computed with the DDB'3Y1-FETAL interaction for the $^{16}O +^{16} O$ system is shown in Figure 2 to have an attractive direct component (upper region), $V_D(E,R)$ and a beautiful exchange component (middle region), $V_{EX}(E,R)$. The total real folded potential resulting from the direct and exchange contributions at incident energies from 10 to 90 MeV/nucleon, being deep and attractive, is shown in Figure 2 to exhibit the same behavior in a nuclear reaction as in (Khoa et al., 1994; Ochala et al., 2021) at smaller inter-nuclear distances. The energy dependence of the total real folded potential is seen in this Figure to come chiefly from the exchange term, which dominates at smaller inter-nuclear distances, especially at low energies, showing that the density-dependent contribution from $V_{EX}(E,R)$ is also much stronger than that from $V_D(E,R)$. But, as the overlap density decreases exponentially in the surface region, the magnitude of $V_{EX}(E,R)$ becomes comparable and even less than that of $V_D(E,R)$, so the total optical potential is being dominated by the direct component at distances R > 7fm. This corroborates that a simple zero-range folding model (Trache et al., 2000; Panda et al., 2014) has been very successful in cases where elastic scattering data is only sensitive to the tail of the optical potential.

It is also evident from Figure 2 that the exchange potential becomes less dominant with increasing incident energy so that both the exchange and direct potentials have about the same strength even at small distances. This makes the total optical potential increasingly repulsive with the incident energy. This finding agrees well with the results of (Khoa et al., 1994; Ochala et al., 2021).

Comparing the optical potential in Figure 2 with the one in Figure 3, one sees that the basic difference between them is that the B'3Y-Fetal-based optical potential has an attractive direct component. In contrast, the real folded potential derived from the B3Y-Fetal has a direct repulsive element (Figure 3), which combines with a very large attractive exchange component to produce an attractive total real folded potential. This difference is a clear manifestation of the effect of mass dependence on the two effective interactions; and it is likely to determine the response and performance of each effective interaction in nuclear reactions involving different nuclear systems. In terms of strength, the results of computation have shown that the optical potential computed with the DDB'3Y1-Fetal potential at the incident energies of 160, 480, 960 and 1440 MeV
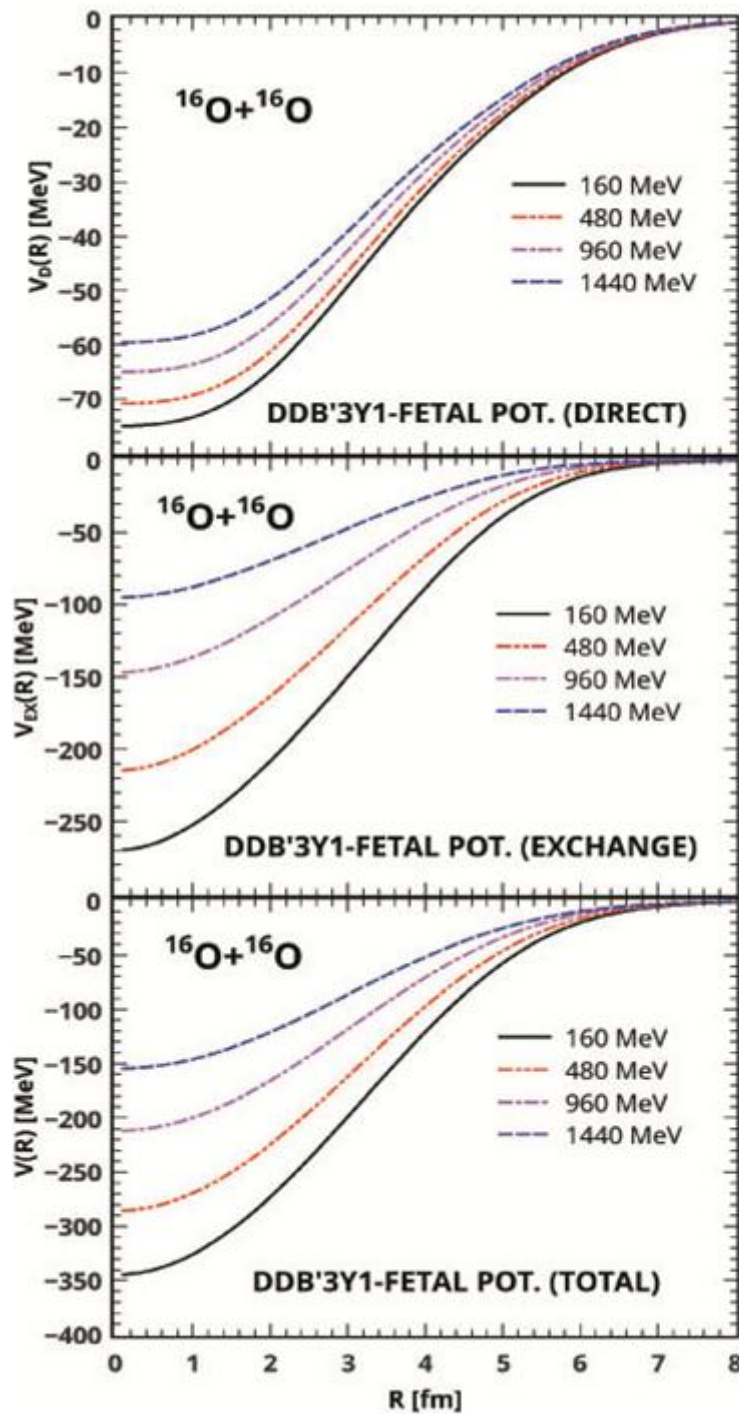
**Figure 2:** Direct (upper part) and Exchange (Middle) Contributions to the Total Folded DDB'3Y1-FETAL Potential (Lower Part) for the $^{16}$O + $^{16}$O System at Incident Energies from 10 to 90 MeV/Nucleon.
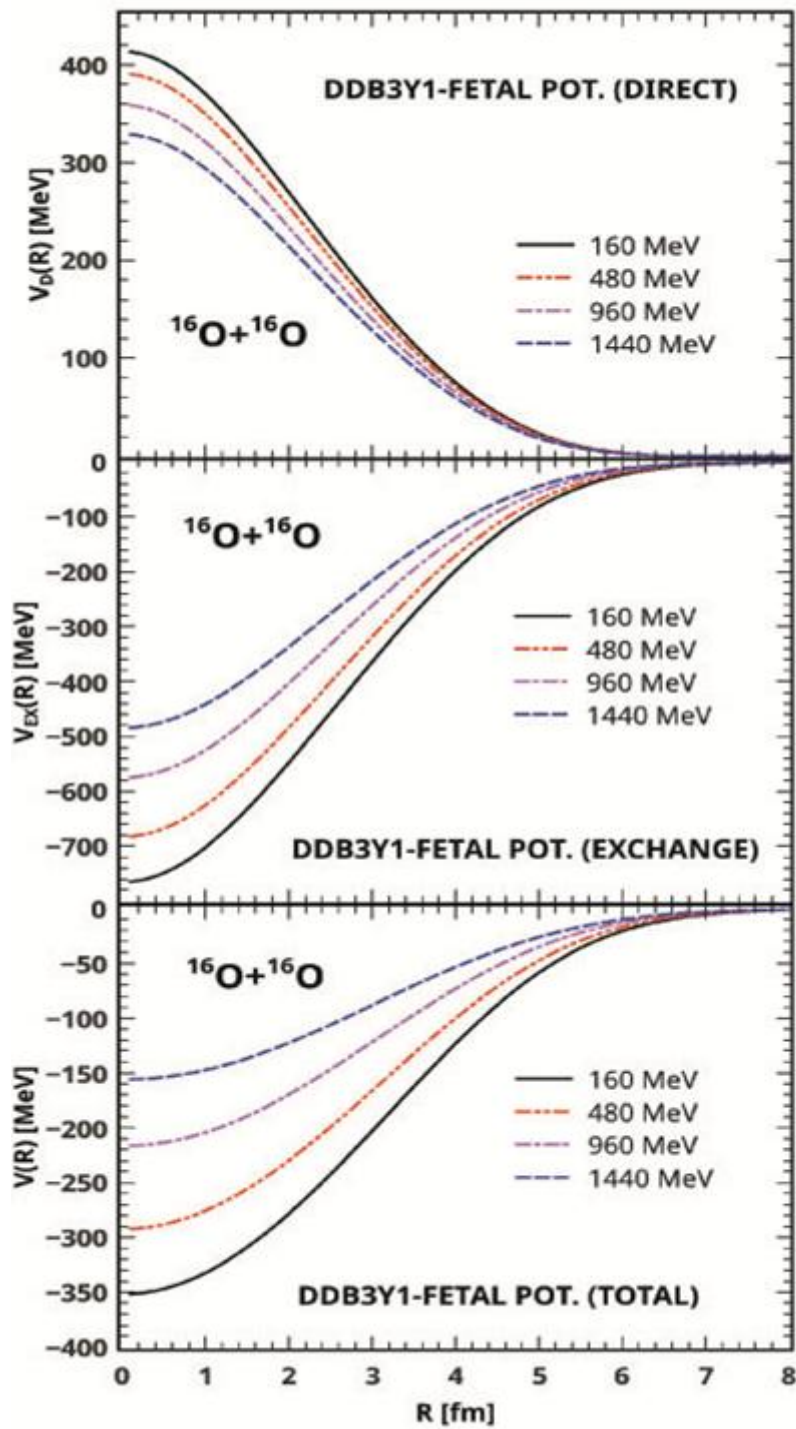
**Figure 3:** Direct (upper part) and Exchange (Middle) Contributions to the Total Folded DDB3Y1-FETAL Potential (Lower Part) for the $^{16}$O + $^{16}$O System at Incident Energies from 10 to 90 MeV/Nucleon
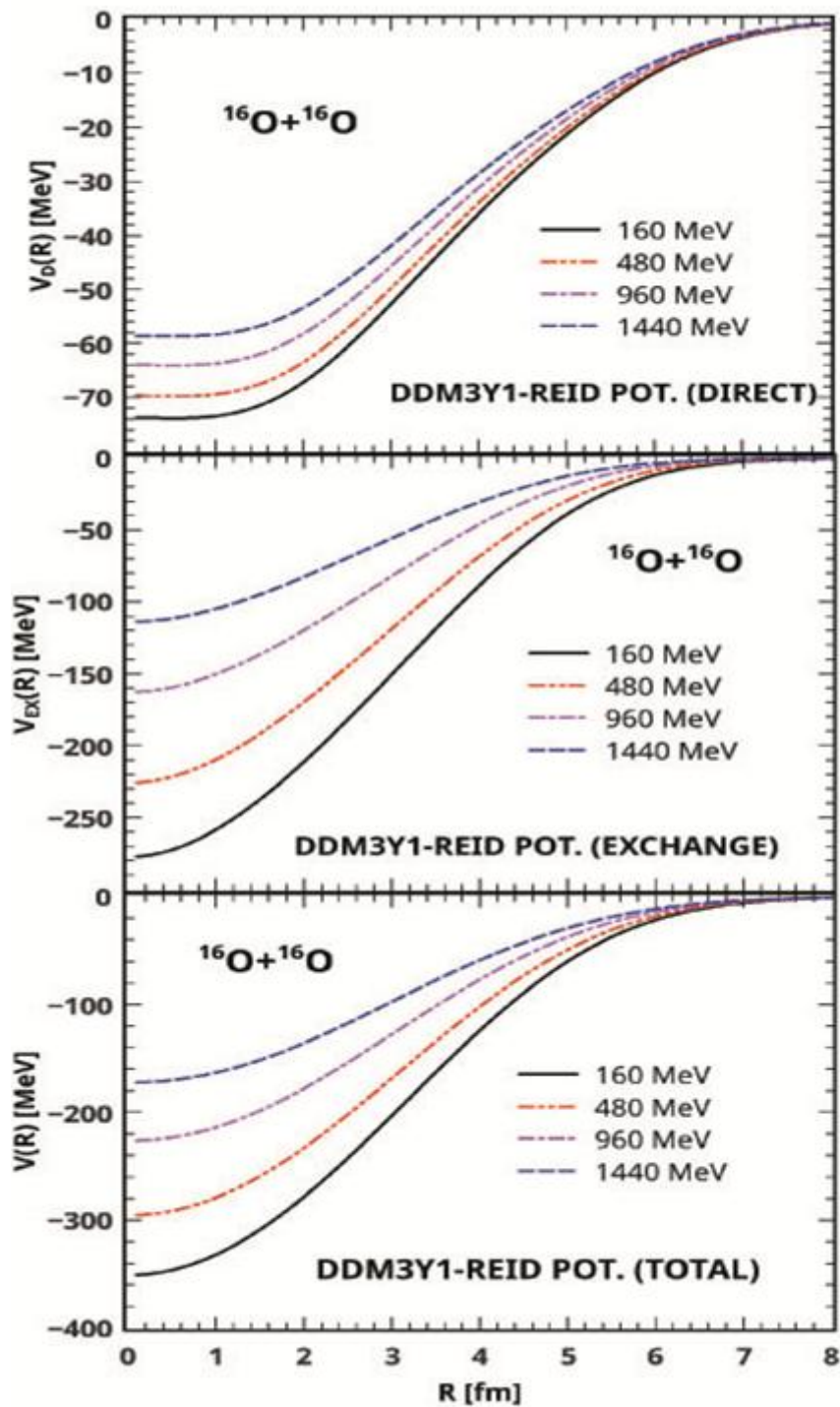
**Figure 4:** Direct (upper part) and Exchange (Middle) Contributions to the Total Folded DDM3Y1-REID Potential (Lower Part) for the $^{16}$O + $^{16}$O System at Incident Energies from 10 to 90 MeV/Nucleon.
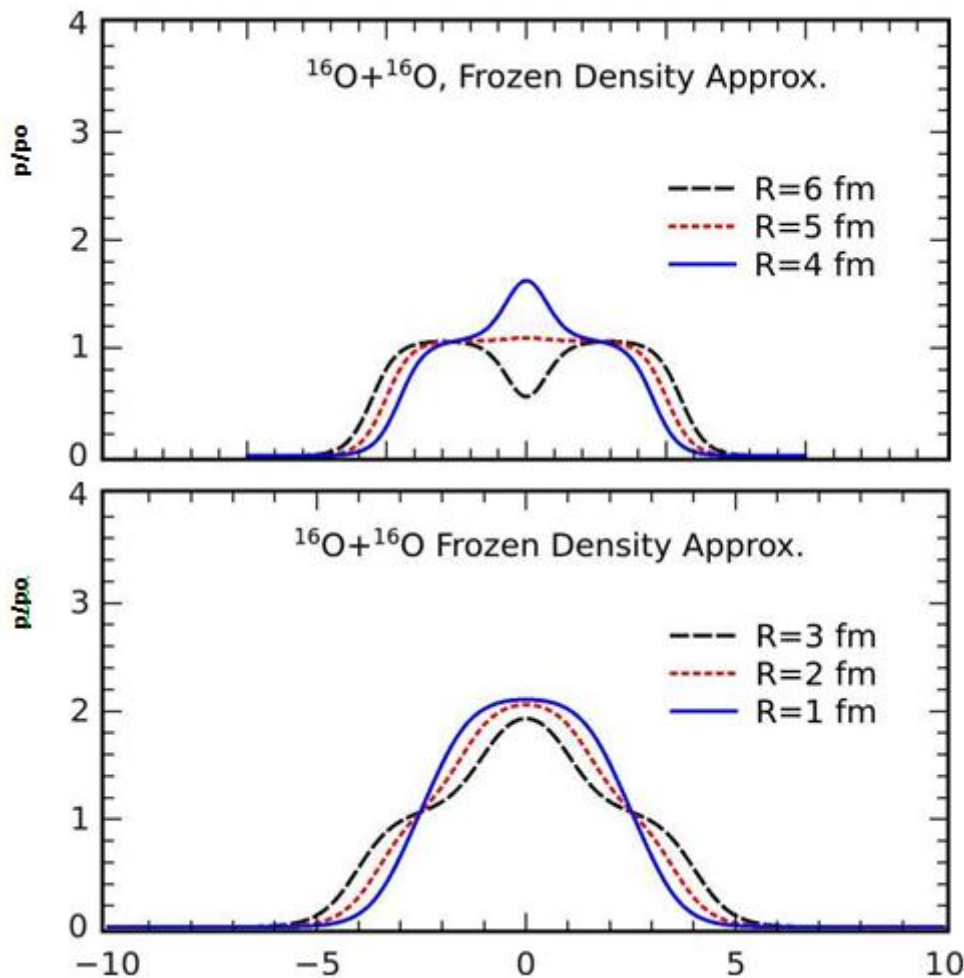
Figure 5: The Overlap Density in the $^{16}O+^{16}O$ System at Different Internuclear Distances Obtained Within the Frozen Density Approximation (FDA)

(Figure 2) at smaller inter-nuclear distances is -345, -289, -212 and -155 MeV in magnitude in comparison with -352, -292, -217 and -156 MeV, respectively, obtained with the DDB3Y1-Fetal real folded potential at the same incident energies, showing the B3Y-Fetal to be stronger at smaller inter-nuclear distances than the B'3Y-Fetal effective interaction. However, the difference between the magnitudes of the two optical potentials is seen to decrease with increasing incident energy. Thus the differences of -7, -3, -5, and -1 MeV between the two optical potentials at the incident energies of 160, 480, 960 and 1440 MeV, respectively, give a clear indication that the strength of the optical potential based on the B3Y-Fetal decreases faster with increasing incident energy than that of the B'3Y-Fetal, meaning that the former becomes more rapidly repulsive than the latter as the incident energy increases; and this in agreement with the findings of (Ochala et al., 2021a).

Finally, Figure 4 is included in this work to show the agreement between the optical potentials based on the M3Y-Reid and B'3Y-Fetal effective interactions. Figure 4 shows that the M3Y-Reid-based real folded potential has an attractive direct component like the B'3Y-Fetal-based optical potential in Figure 2. Based on this similarity, it is hoped that the behaviour of the optical potential derived from the B'3Y-Fetal might have some resemblance to that of M3Y-Reid more than the B3Y-Fetal effective interaction in the elastic scattering of some nuclear systems. Future studies on elastic scattering involving these interactions will certainly produce far-reaching insights into this matter. Certainly, the similarity between the optical potentials of these effective interactions is convincing evidence of the viability of the B'3Y-Fetal in nuclear reactions and the validity of the LOCV method used for its derivation.

In summary, the application of the B'3Y-Fetal interaction to nuclear reaction has provided insightful information about its nature, character, performance strengths in comparison with the B3Y-Fetal. An important point worth mentioning which is a major contribution in this paper is that these interactions are mass-dependent, which shows up as one goes up from one nuclear system to another as reported in (Ochala et al, 2020). The precise manifestation of mass dependence revealed in this study is that although they were derived based on the LOCV model and have the same functional form (Equation 1), the direct component of the optical potential derived from the B'3Y-Fetal (A = 24) is attractive, whereas the B3Y-Fetal-based (A = 16) optical potential has a repulsive direct component. This revealed fact is a major novel finding in this work. The resemblance of the B'3Y-Fetal-based

optical potentials to those based on the M3Y-Reid is convincing evidence of the viability of this new mass-dependent effective interaction and the validity of LOCV method used for its derivation.

## The Overlap Density

The folding calculation results have shown that the overlap density of the two colliding nuclei has its highest point at small inter-nuclear distances. Figure 5 presents the overlap density obtained for the $^{16}O + ^{16}O$ system within the frozen density approximation; and it represents the high density of matter formed during collisions at different impact parameters. This figure shows that the density buildup is highest at 1 fm and lowest at 6 fm.

At inter-nuclear distances between 2 fm and 3 fm, the density build-up grows well above the normal nuclear matter density to about $2\rho_0$. These findings are in good agreement with the results obtained by Khoa and his co-researchers Khoa et al., 1994).

## CONCLUSION

The new mass-dependent effective interactions, the B'3Y-Fetal and B3Y-Fetal effective interactions derived based on the LOCV method (Fiase et al., 2002) from the nuclear systems, A = 24 and 16 respectively, have been applied to nuclear reactions involving $^{16}O+^{16}O$ at different incident energies within the framework of the double folding model to solely determine and compare the form and character of the first with the second interaction in this paper. This study's major, novel findings are summarized in the following concluding statements.

- Folding calculation is observed to be a computational necessity for a complete description of the form and character of the B'3Y-Fetal in comparison with the B3Y-Fetal effective interaction. Figure 2 gives clear, convincing information about the form and character of the B'3Y-Fetal that nuclear matter calculations in (Ochala et al., 2020) could not provide. Even though the two effective interactions were derived using the same theoretical model, the lowest order constrained variational approach. Due to their mass dependence, they are shown not to have exactly the same form and character in the nuclear reaction. This is conclusive evidence of the effect of mass dependence on the two effective interactions provided by folding analysis.
- The total real folded potential based on the B'3Y-Fetal combines attractive direct and exchange components. In contrast, the B3Y-Fetal-based real folded potential has a direct repulsive element, which combines with a significant attractive exchange component to form an attractive, total real optical potential. Therefore, the clear fundamental difference between them, in terms of form and character, is the fact that the visual potential derived from the B'3Y-Fetal has an attractive direct component while that of the B3Y-Fetal interaction has a direct repulsive element; and this is a clear manifestation of the effect of mass dependence.
- The optical potential based on the B3Y-Fetal effective interaction has been observed to grow more rapidly repulsive with increasing incident energy than the one based on the B'3Y-Fetal effective interaction, in agreement with the findings of (Ochala et al, 2021a)..
- The optical potential derived from the B'3Y-Fetal has been found to be similar, in form, to the optical potential based on the M3Y-Reid effective interaction shown in Figure 4. The M3Y-Reid-based optical potential has an attractive direct component, which combines with an attractive exchange component to form an attractive total real folded potential in the same way that the B'3Y-Fetal-based optical potential is a combination of attractive direct and exchange components. This finding shows that the optical potentials derived from the B'3Y-Fetal will likely behave more like the those based on the M3Y-Reid than the B3Y-Fetal effective interaction in nuclear reactions.
- The heavy-ion optical potential derived from the B'3Y-Fetal has been found to be deep and attractive at small inter-nuclear distances, especially at low energies, as shown in Figure 2. This indicates the possibility of using this mass-dependent effective interaction in the refractive scattering of nuclear systems with positive results.

Finally, the findings of this study have revealed the basic difference, in form and character, between the B'3Y-Fetal and B3Y-Fetal effective interactions. Furthermore, nuclear matter (Ochala et al., 2020) and folding calculations have conclusively established these two effective interactions. Indeed, the most viable of the four mass-dependent effective interactions derived based on LOCV method (Fiase et al., 2002).

Hopefully, the findings herein do endorse that they will be of good use in nuclear reactions as well as in Nuclear Astrophysics (Chien et al., 2018; Anh et al., 2020) where nuclear EOS is a major ingredient in calculations; certain nuclear reactions are the main probe of exotic nuclear species; and accurate knowledge of nuclear reaction rates needed for understanding primordial nucleosynthesis and hydrostatic burning in stars requires a combination of new experimental techniques and theoretical efforts.

## ACKNOWLEDGEMENTS

## COMPETING INTERESTS

All authors agree that this paper should be published in the Australian Journal of Basic and Applied Sciences. This paper has not been recently submitted to any journal for publication; therefore, there are no competing interests.

### Authors' Contributions
First Author: Conceptual design of research and manuscript preparation.
Second Author: Conceptual design of research and supervision of manuscript preparation.
Third Author:  Proofreading and editing of manuscript.
Fourth Author:  Proofreading and editing of manuscript.
All authors participated in the editing of the paper in the revised form.

## REFERENCES

Anh, N. L., N. H. Phuc, D. T. Khoa, L. H. Chien, and N. T. T. Phuc, 2021. Folding Model Approach to the     Elastic $p+^{12,13}$C Scattering at Low Energies and Radiative Capture $^{12,13}$C(p,γ) Reactions. Nuclear Physics A. 1006(122078).     DOI: 10.1016/j.nuclphysa.2020.122078.

Bohr A. A. and Mottelson B. R., 1969. Nuclear Structure, Volume 1: Single     Particle Motion. W.A Benjamin Inc. Amsterdam. 471P.

Brieva F. A., and J. R. Rook, 1977. Nucleon-Nucleus Optical Model (1). Nuclear     Matter Approach. Nuclear Physics A.291: 299 - 316 DOI:10.1016/0375-9474(77)90322-0.

Chien L. H., D. C. Cuong, and D. T. Khoa, 2015. Mean- Field Study of $^{12}$**C** + $^{12}$**C**     Fusion. Communications in Physics. 25(3): 265-274 DOI:10.15625/0868- 3166/25/3/7427.

Chien L. H., D. T. Khoa, D. C. Cuong, N. H. Phuc, 2018. Consistent Mean- Field Description of the $^{12}$C + $^{12}$C Optical Potential at Low Energies and the Astrophysical S-Factor. Physical Review C. 98(064604). DOI:10.1103/PhysRevC.98.064604.

Colo G., and N. V. Giai, 2004. Theoretical Understanding of the Nuclear Matter     Incompressibility: Where Do We Stand? Nuclear Physics A. 731: 15 - 27. DOI: 10.1016/j.nuclphysa.2003.11.014.

Fiase J. O., K. R. S. Devan, and A. Hosaka, 2002. Mass Dependence of M3Y-Type Interactions and the Effects of Tensor Correlations. Physical Review C. 66(014004): 1 - 9. DOI:10.1103/PhysRevC.66.014004.

Gontcharn, I., D. J. Hinde, M. Dasgupta, and J. O. Newton, 2004. Double Folding     Nucleus-Nucleus Potential Applied to Heavy- Ion Fusion Reactions. Physical     Review C. 69(024610): 1-14. DOI:10.1103/PhysRevC.69.02461.

Hamada, S., N. Burtebayev, N. Amangeldi, K. A. Gridnev, K. Rusek, Z. Kerimkulov, and N. Maltsev, 2012. Phenomenological and Semi- Microscopic Analysis for $^{16}$O and $^{12}$C Elastically Scattering on the Nucleus of $^{16}$O and $^{12}$C at Energies Near Coulomb Barrier. Journal of Physics: Conference Series. 381(12130): 1 - 6. DOI: 10.1088/1742- 6596/381/1/012130.

Khoa, D. T., V. W. Oertzen, and H. G. Bohlen, 1994. Double-Folding Model for Heavy-ion Optical Potential: Revised and Applied to Study $^{12}$C and $^{16}$O Elastic Scattering. Physical Review C. 49(3): 1652 - 1667. DOI:1103/PhysRevC.49.

Khoa, D. T. and V. W. Oertzen, 1995. Refractive Alpha-Nucleus Scattering; A Probe for the Incompressibility of Cold Nuclear Matter. Physics Letters 342: 6 - 12. DOI: 10.1016/0370-2693(94)01393-Q.

Khoa, D. T. K., N. H. Phuc, T. L. Doan, and M. L. Bui, 2016. Nuclear Mean     Field and Double-Folding Model of the Nucleus-Nucleus Optical Potential.     Physical Review C. 94(034612): 1 - 16. DOI: 10.1103/Phys- RevC.94.034612.

Loan, T. L., M. L. Bui, and D. T. Khoa, 2015. Extended Hartree-Fock Study of the Study of the Single-Particle Potential: the Nuclear Symmetry Energy, Nucleon Effective Mass and Folding Model of the Nucleon Optical Potential. Physical Review C., 80(011305(R)): 1 - 16. DOI: 10.1103/PhysRevC.92.034304.

Ochala, I. and J. O. Fiase, 2018. Symmetric Nuclear Matter Calculations - A     Variational Approach. Physical Review C. 98(064001): 1-8.     DOI:10.1103/PhysRevC.98.064001.

Ochala, I., F. Gbaorun, J. A. Bamikole, and J. O. Fiase, 2019. A microscopic Study of Nuclear Symmetry Energy with an Effective Interaction Derived from Variational Calculations. International Research Journal of Pure and Applied Physics. 6(2): 22 - 33.

Ochala, I., J. O. Fiase, H. O. Momoh, and I. C. Okeme, 2020. The Mass- Dependent Effective Interactions as Applied to Nuclear Matter. Nigerian Journal of Physics. 29(1): 209 - 219.

Ochala, I., D. Terver, and J. O. Fiase, 2020a. A Study of $^{12}$C+$^{12}$C Nuclear Reaction using a New M3Y-Type Effective Interaction. International Journal of Physics Research and Applications. 3: 133 - 142. DOI:10.29328/journal.ijpra.1001031.

Ochala, I., 2021. optical Model Analyses of Elastic Scattering of $^{16}$O+$^{12}$C. International Journal of Applied Mathematics and Theoretical Physics. 7(1): 1 - 9. DOI: 10.11648/j.ijpra.20210701.11

Ochala, I., and J. O. Fiase (2021a). B3Y-Fetal Effective Interaction in the Folding  Analysis of Elastic Scattering of $^{16}O +^{16}O$. Nuclear Science and Techniques. 32(8): 1 – 14. DOI: 10.1007/s41365-021-00920-z.

Panda, K.C, B.C. Sahu, and J. Bhoi, 2014. Accuracy of Simple Folding Model in the Calculation of the Direct Part of Real $a — a$ Interaction Potential. PRAMANA Journal of Physics. 82(5): 841 - 849. DOI:10.1007/s12043-014-0737-2.

Shlomo S., and D. H. Youngblood, 1994. Nuclear Matter Incompressibility and  Giant Monopole Resonance. Nuclear Physics A. 569: 303 - 312.          DOI:10.1016/0375-9474(94)90121-X.

Tan N. H., T. L., D. T. Khoa, and D. T. Loan, 2021. Equation of State of Asymmetric Nuclear Matter and the Tidal Deformability of Neutron. The European Physical Journal A.  57(4): DOI: 10.114/epja/s10050-021-00467-y.

Trache, L., A. Azhari, H. L. Clark, C. A. Gagliardi, W. Lui, A. M.     Mukhamedzhanov, R. E. Tribble, and F. Carstoiu, 2000. Optical Model Potential Involving Loosely Bound p-Shell Nuclei Around 10 Mev/ nucleon. Physical Review C. 61(024612):1 - 15. DOI:10.1103/PhysRevC.61.024612.